Calcium carbonate activated biomass-derived carbon: insights on characterization and adsorption

R. Sangeetha Piriya, Rajamani M. Jayabalakrishnan*, M. Maheswari, Kovilpillai Boomiraj and Sadish Oumabady

Department of Environmental Sciences, Tamil Nadu Agricultural University, Coimbatore 641 003, India

Activated carbon made from coconut (*Cocos nucifera*) shells has the potential to be a valuable source for removing pollutants from wastewater. Recently, the use of calcium carbonate to activate carbon materials derived from agricultural waste has been gaining attention as an effective method for adsorption in wastewater treatment. In the present study, we have analysed the structural and functional properties of activated coconut shell biochar. Results show that calcium carbonate-activated carbon had a maximum adsorption capacity of 40.35 mg g^{-1} after 3 h of equilibrium when tested with 20 mg l^{-1} of malachite dye. The R_2 value for this activated carbon was 0.822, and the best-fit model was determined to be pseudo-second-order kinetics, with intraparticle diffusion being the final rate-limiting step.

Keywords: Agricultural waste, calcium carbonate activation, coconut shell, wastewater treatment.

DYES cause severe problems for living beings when discharged into the environment. Synthetic dyes are resistant to chemical and biological degradation. Dyes are useful for various purposes, but once released into the aquatic biota, they become a matter of serious concern. Malachite green is basically a cationic dye widely used as an additive and colourant in industrial applications such as paper, silk and leather[1]. Exposure to malachite green dye at low concentrations causes various health effects through inhalation and ingestion. Carcinogenicity, mutagenicity, teratogenicity and infertility in humans have been reported due to exposure to this dye[2]. The removal of malachite green is essential to eliminate health and environmental threats. Therefore, a successful treatment process should be carried out before discharging dye wastewater into the streams. Several methods have been employed for the treatment of dyes from wastewater such as coagulation[3], advanced oxidation[4], membrane technology[5] and adsorption techniques[6]. Dye wastewater treatment using adsorption techniques is found to be more effective and versatile compared to other methods. Researchers have tested the efficacy of adsorbents for the removal of dyes from industrial wastewater. The success of adsorption depends on the capacity and surface affinity of the adsorbent towards the dye molecules. The eco-friendly adsorbents include agricultural biomass and modified products. Industrial waste, microbial biomass or natural polymers are also used in the removal of dyes from wastewater. The removal of dyes from wastewater is still an emerging field of study for researchers.

Pollachi district, Tamil Nadu, India, is a major coconut-producing region due to the prevailing ambient climatic conditions in the shadows of the Western Ghats. The agricultural waste generated from the coconut fields is either burned or dumped in landfills. Therefore, the concept of value addition can reduce a huge volume of waste, effectively enabling both solid-waste management and the circular economy. After Karnataka, Tamil Nadu accounts for 4.44 lakh hectares with 11,526 nuts per hectare. About 60–65% of the coconut fruit is generated as waste[7]. The coconut industry generates a relatively large amount of coconut shell and husk biomass, which can be utilized for industrial and environmental purposes. The abundant and readily available coconut shells can be effectively utilized as a source of energy[8]. The conversion of coconut shells to activated carbon (AC) is a cheap and best alternative to other commercial carbon sources.

The cost-effectiveness of adsorption using activated carbon is a significant challenge. In recent years, researchers have primarily focused on using agricultural waste to produce activated carbon as an alternative to commercially available options. While there have been a lot of studies on producing activated carbon using chemical activating agents such as zinc chloride, sulphuric acid and phosphoric acid, there has been limited research on using calcium carbonate as an activating agent[9–13]. The aim of this study was to analyse the activation of coconut shells using calcium carbonate and to understand the malachite green dye adsorption mechanism using this type of activated carbon.

Materials and methods

Adsorbent carbon

Coconut shells (Coconut ALR (CN) 3 variety) for this study were collected from the Coconut Research Station (CRS),

*For correspondence. (e-mail: jayabalphd@gmail.com)

Tamil Nadu Agricultural University, Coimbatore. The shells were sun-dried and subjected to carbonization at 450°C in a slow pyrolysis unit. The carbonized material was crushed, sieved (0.2 mm) and stored in an airtight PTFE container for a week for further studies.

$CaCO_3$ activated carbon

Calcium carbonate (analytical grade) was purchased from M/s Sigma Aldrich (Merck, India). AC was activated over a layer of powdered $CaCO_3$ in a closed graphite crucible at 550°C for 30 min, followed by thermal activation at 750°C for 30 min. The activated material was washed using distilled water 3–4 times, oven-dried at 110°C for 6 h, sieved and stored in an airtight container for further studies[14].

Characterization of AC and Ca-AC

The pH and electrical conductivity (EC) of AC and $CaCO_3$ activated carbon (Ca-AC) were determined using a pH meter and EC meter respectively. The volatile matter, moisture content and ash content were estimated using standard ASTM protocols (ASTM-D3175-07, ASTM-E871-82 and ASTM-D3174-04). Ultimate analysis (C, H, N, S and O) was carried out using an elemental analyser (Elementar Vario EL III). The thermogravimetric/differential scanning calorimetry (TGA/DSC) analysis was carried out using a thermal analyser (Perkin Elmer simultaneous thermal analyser STA 6000)[11]. The functionalities of AC and Ca-AC were identified using the Fourier-transform infrared spectroscopy (FTIR; Model 8400 S, Shimadzu, Japan) over the wavenumber range (400 to 4000 cm^{-1})[11]. The surface morphology and features of AC and Ca-AC were examined using a scanning electron microscope (SEM) with energy dispersive X-ray (EDX) microanalysis (FEI-Quanta 250, Czech Republic) and transmission electron microscope (TEM; FEI-Quanta 250)[15]. The Brunauer–Emmett–Teller (BET) surface area analysis of AC and Ca-AC was performed using a BET surface area analyser (Smartsorb 92/93). The particle size and zeta potential of AC and Ca-AC were determined using a particle size analyser (Horiba Scientific Nanopartica SZ-100)[16].

Batch adsorption studies

Experiments were conducted in batches at 25° ± 2°C using varying concentrations of malachite green dye (20, 35, 50, 65, 80 mg l^{-1}) and 4 g l^{-1} of AC and Ca-AC at specific time intervals (20, 40, 60, 80, 100, 120, 140, 160, 180, 200 and 220 min) with continuous agitation provided by an orbital shaker at 210 rpm. Adsorption isotherms and kinetic studies were performed for malachite green dye concentrations between 20 and 80 mg l^{-1}. The malachite green dye was obtained from Sigma-Aldrich (Germany), and the UV–Vis spectrophotometer (Shimadzu UV-1800) at 618 nm was used to quantify the dye after centrifugation at 6000 rpm for 10 min, and subsequent filtration to separate the solid and liquid portions of the experiment[17].

Results and discussion

Characterization of AC and Ca-AC

Table 1 gives the physico-chemical properties of AC and Ca-AC. The alkaline pH of AC (8.79) and Ca-AC (8.30) was due to the accumulation of alkaline functional groups (carboxyl, hydroxyl and amino groups) during the carbonization process with simultaneous loss of hydrogen and oxygen from the feedstock irrespective of the speciation. The activation process resulted in a lower electrical conductivity for Ca-AC (0.15 dS m^{-1}) compared to AC (1.70 dS m^{-1}) due to the leaching of salts[18]. Proximate analysis revealed a change in the proportion of AC components after thermal treatment. AC had a higher volatile matter content (70.57%) compared to Ca-AC (19.50%). This significant decrease in volatiles was a result of the elimination of all non-carbon labile compounds[19]. The fixed carbon increased from 17.39% (AC) to 75.50% (Ca-AC). The carbonization process had a significant impact on the volatile matter in terms of yield and porosity for Ca-AC, compared to AC. As a result, there was a slight decrease in yield recovery for both AC (50.4%) and Ca-AC (47.20%)[20]. The elemental composition of AC after $CaCO_3$ activation showed an increase in the oxygen content of Ca-AC (15.11%). The sulphur content was negligible (0–0.11%), and the carbon content was 72.27% for AC and 78.01% for Ca-AC. The increase in carbon content was due to dehydration, decarboxylation and condensation reactions[18]. The formation of oxygen functional groups on the surface was observed by measuring the zeta potential of AC (–24.2 mV)

Table 1. Properties of coconut shell carbon and activated carbon

Parameters	Adsorbent carbon (AC)	$CaCO_3$ activated carbon (Ca-AC)
pH	8.79	8.30
Electrical conductivity (dS m^{-1})	1.70	0.15
Proximate analysis		
Moisture content (%)	1.50	1.56
Volatile matter (%)	79.57	19.50
Ash content (%)	1.35	3.90
Fixed carbon (%)	17.39	75.05
Ultimate analysis		
Nitrogen (%)	5.48	0.28
Carbon (%)	72.27	78.01
Sulphur (%)	0.11	ND
Hydrogen (%)	12.12	2.70
Oxygen (%)	9.13	15.11
Yield recovery (%)	50.4	47.2
BET surface area (m^2 g^{-1})	45.6	223.77
Zeta potential (mV)	–24.2	–24.6

and Ca-AC (–24.6 mV), indicating a negative surface charge[21].

FTIR analysis

Figure 1 shows the FTIR spectra of AC and Ca-AC. The aliphatic and alkane group (C–H stretching) stretching vibrations were indicated by the wide band at 2916.81 cm^{-1} on Ca-AC after activation. Functional groups of alcohol, acids, phenols or esters are generally found vibrating on the activated carbon surface[22]. Both AC and Ca-AC had a C–C stretching vibration of aromatic rings at 1579.41 and 1576.52 cm^{-1} respectively. The peaks observed at 1159.01 cm^{-1} and 1026.91 cm^{-1} were determined to be from the C–O stretching of the secondary alcohol group. The band at 437 cm^{-1} was identified as C–Cl stretching, which is a result of the presence of chlorine atoms on the surface, as indicated by the EDX analysis of Ca-AC (ref. 23). The vibrations of the functional groups at 437, 1528 and 1062.91 cm^{-1} play a role in the adsorption of malachite green molecules onto Ca-AC (ref. 24). The FTIR results of the activated carbon were consistent with those of other activated carbons produced from biomass sources such as walnut shell[25], salvia seeds[26], wood apple shell[27] and potato stem powder[28].

SEM-EDX analysis and TEM analysis

Figure 2 depicts the SEM photomicrographs of AC and Ca-AC. The elliptical pores were observed on the surface of AC ranging from 2.2 to 10.12 µm. An increase in the dense network of widened heterogeneous pores on Ca-AC can be observed in the figure. The development of a porous surface on activated carbon is also observed under SEM showing numerous cracks and crevices within nanometre dimensions. The nanosized pores range from 714 to 821 nm. CO_2 is released when calcium carbonate is carbonized at a higher temperature. The excessive release of CO_2 will create a favourable atmosphere for the reaction of all active sites and the formation of pores[11]. A noticeable impact of carbonization at 450°C can be seen by eliminating the volatiles from AC, resulting in cavity production on the surfaces[29]. The continuous emission of CO_2 can cause the formation of unfavourable pores, which can result in carbon burning[30]. The SEM photomicrograph of almond peel before malachite green dye adsorption showed a similarly wide, porous surface indicating its good adsorbing capacity[24]. The irregular pores show better interaction between the gas and activated carbon through the diffusion of CO_2 molecules, resulting in significant pore formation[31]. EDX microanalysis was performed to identify the elemental composition of AC and Ca-AC. It detected the percentage element present in the following order: C (87.85) > O (10.87) > Cl (0.58) > P (0.38) > Si (0.33) (Figure 2). After activation, the presence of elements was found in the following order: C (85.31%) > O (09.96%) > Na (1.11%) > Mg (0.83%) > Ca (0.54%) > K (0.53%) > Si (0.51%) > Al (0.39%) > Cl (0.35%) > P (0.30%).

The visualization of TEM images of AC and Ca-AC revealed their internal structures (Figure 3). The size of AC and Ca-AC was found to range from 46.4 to 91.3 nm and 26.9 to 36.9 nm respectively.

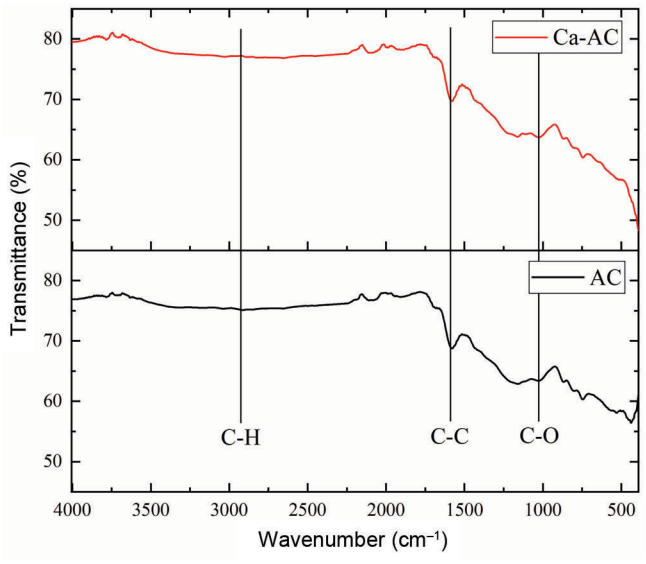

Figure 1. FTIR spectra of adsorbent carbon (AC) and $CaCO_3$ activated carbon (Ca-AC).

TGA/DSC analysis

The TGA/DSC curves for AC and Ca-AC showed percentage weight loss (Figure 4). The weight loss was observed between 32% and 91% during different stages of decomposition when the temperature increased from 300°C to 800°C. The initial stage of decomposition at 100°C was due to water removal, 110°–200°C represented the removal of volatiles, and 200°–450°C showed the decomposition of cellulosic materials. The obtained profiles showed oxygen-containing functional groups released from AC (refs 32, 33). The curves obtained for Ca-AC showed weight loss above 500°C resembling the thermal decomposition of $CaCO_3$. This analysis was similar to the TG/DSC analysis of activated biochar of *Opuntia ficus-indica*[11].

BET analysis

The BET surface area of AC was 45.6 sq. m/g. After being activated with calcium, the BET surface area of Ca-AC (223.77 sq. m/g) was found to be higher than that of regular AC. This increase in surface area could be attributed to the formation of more pores, as revealed by the Ca-AC SEM photomicrograph[34]. The internal walls of the microspore break at 850°C and mesopores develop, leading to a better

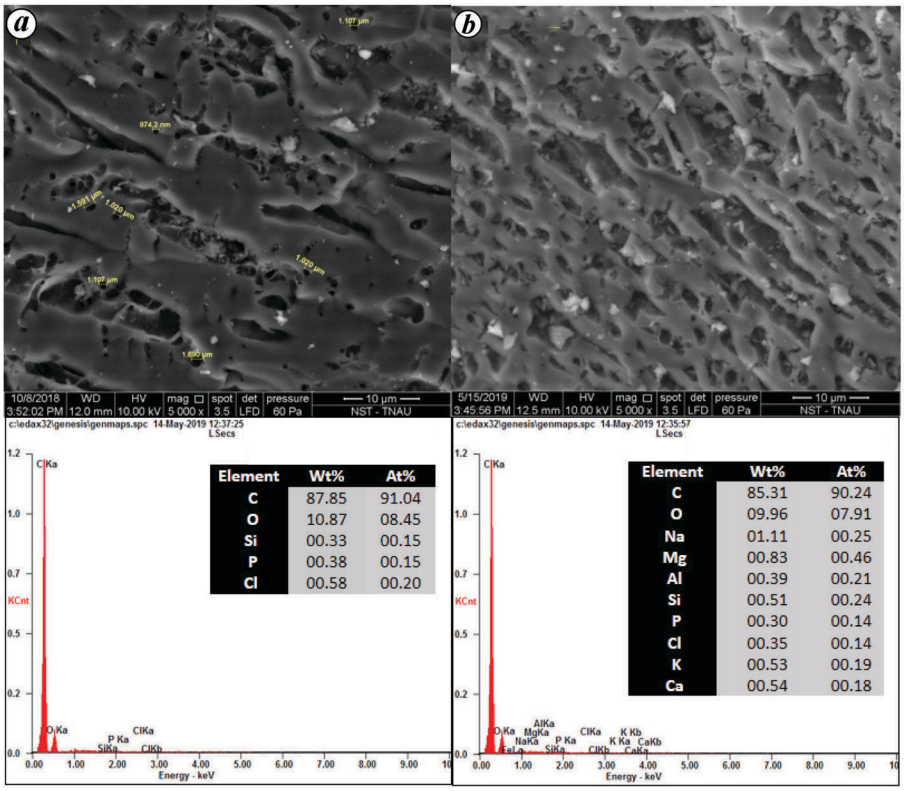

Figure 2. SEM (with EDX) photomicrographs of (***a***) AC and (***b***) Ca-AC.

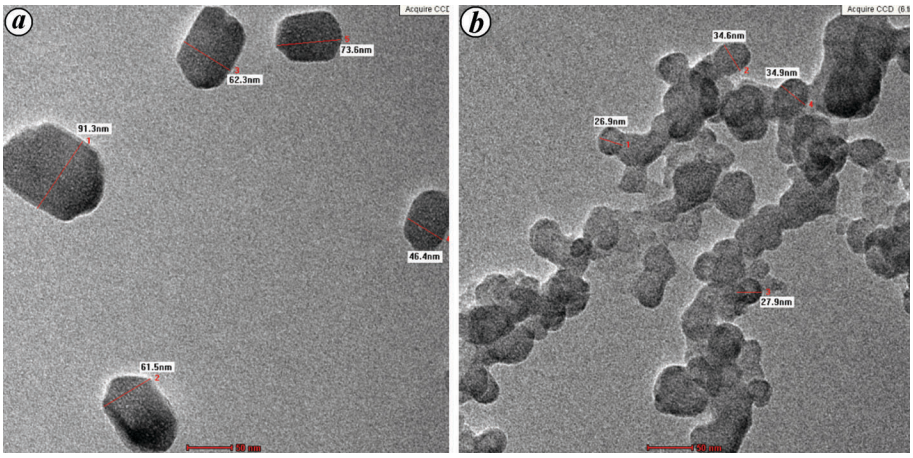

Figure 3. TEM photomicrographs of (***a***) AC and (***b***) Ca-AC at 50 µm.

surface area. However, the results were in contrast to those of iron(III) oxide magnetic nanoparticles (PAC@Fe_3O_4–MN), which had a reduced surface area after undergoing the calcination process[35].

Adsorption isotherm and kinetics

The isotherms of adsorption were studied using Langmuir, Freundlich and Temkin models (Table 2). The experimental results were compared and correlated with the coefficient of determination (R^2) before and after the activation process (Figure 5). The adsorption of malachite green dye on the surface of AC (0.998) and Ca-AC (0.995) strictly followed the Freundlich isotherm model, which depicted the multilayer coverage of dye molecules on their surface. The maximum adsorption of malachite green dye (X_m) was 54.35 and 40.65 mg g^{-1} respectively, for AC and Ca-AC. The Freundlich model illustrated the extent of adsorption by K_f value greater than 1. The K_f values for AC (1.006) and Ca-AC (1.059) were in favour of the adsorption process, indicating a heterogeneous interaction between the

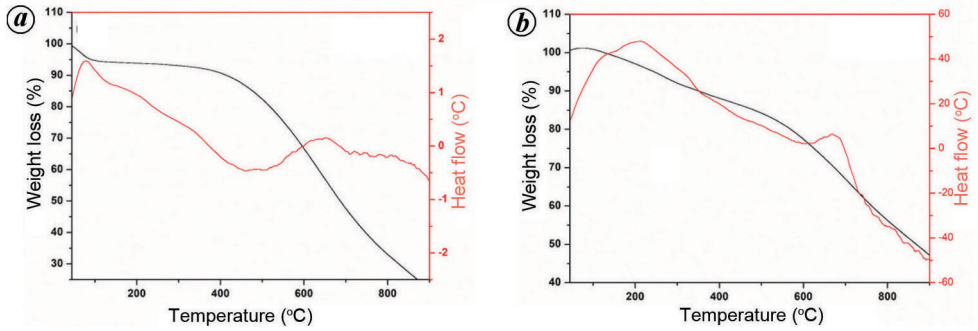

Figure 4. Thermo-gravimetric plots of (***a***) AC and (***b***) Ca-AC.

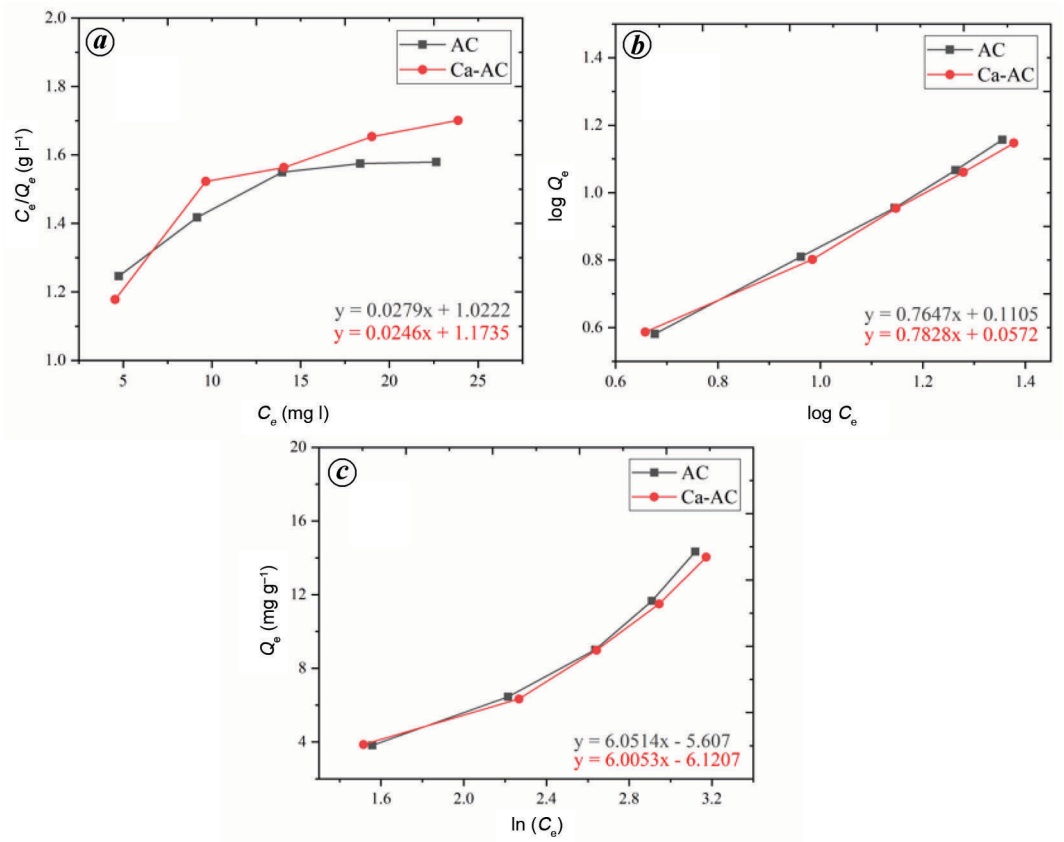

Figure 5. Adsorption isotherm curves: (***a***) Langmuir, (***b***) Fruendlich and (***c***) Temkin models of AC and Ca-AC.

Table 2. Isotherm parameters for malachite green adsorption

	Langmuir equation				Freundlich equation			Temkin equation		
Adsorbent	R^2	X_m	K_l	R_L	R^2	K_f	n	R^2	B	K_t
AC	0.836	54.348	0.022	0.450	0.998	1.006	1.190	0.946	0.381	2.993
Ca-AC	0.825	40.650	0.029	0.460	0.995	1.059	1.277	0.940	0.413	2.771

malachite green dye and the AC surface[36]. Similarly, the value of n (Freundlich isotherm constant) indicated the favourability of the adsorption process. It was found to be favourable ($n > 1$) for AC (1.190) and Ca-AC (1.277). The adsorption of ibuprofen on the surface of coconut husk-activated carbon showed contradictory results, following the Langmuir adsorption model (76.92 mg g^{-1})[36]. Blue-41 dye adsorption on zeolite/Fe_3O_4 nanocomposites indicated the Freundlich model as being favourable[37].

The adsorption kinetics of malachite green dye was examined using pseudo-first-order, second-order, Elovich and intraparticle diffusion models (Table 3). The adsorption

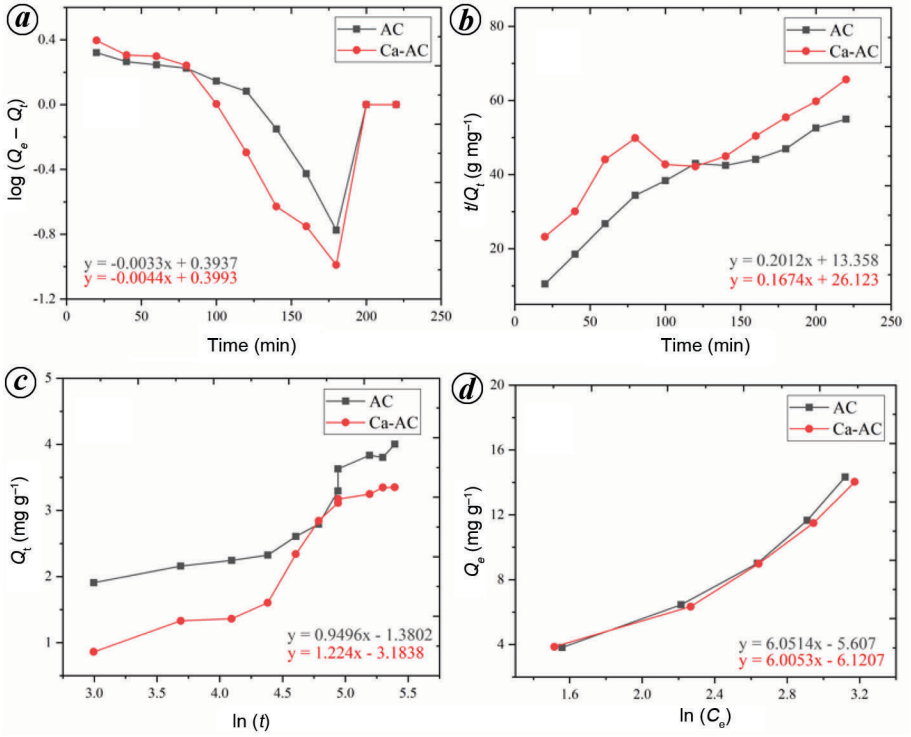

Figure 6. Adsorption kinetic curves: (***a***) pseudo first order, (***b***) pseudo second order, (***c***) Elovich models and (***d***) intraparticle diffusion models of AC and Ca-AC.

Table 3. Kinetic parameters for malachite green adsorption

	Pseudo first order		Pseudo second order		Elovich model			Intraparticle diffusion	
Adsorbent	R^2	K_1	R^2	K_2	R^2	α	δ	R^2	K_i
AC	0.437	0.007	0.920	1.849	0.825	3.858	1.052	0.929	0.627
Ca-AC	0.380	0.010	0.822	1.366	0.900	20.194	0.816	0.938	0.481

Table 4. Different adsorbents used for the removal of malachite green

Adsorbent	Adsorption capacity (mg g^{-1})	Reference
Natural date stone	31.5	17
Natural red clay	84.75	41
Walnut shell	90.8	25
Salvia seeds	19.16	26
Sugarcane bagasse	23.41	42
Wood apple shell	34.56	27
Potato stem powder	27.0	28
Activated carbon (Ca-AC)	40.65	Present study

rate initially increased and then decreased over time (Figure 6). Equilibrium was reached after 3 h, with a maximum adsorption capacity of 40.650 mg l^{-1}. Diffusion occurred in both meso and micropores, indicating internal mass transfer of malachite green dye molecules. As the dye concentration increased from 20 to 80 mg l^{-1}, the efficiency of malachite green adsorption on AC decreased. The available active sites were reduced as the adsorption process reached equilibrium, causing dye molecules to take longer to reach the least accessible sites. The pseudo-first-order kinetic model was not suitable due to a lower R^2, while the pseudo-second-order kinetic model was more suitable (AC – 0.437 and Ca-AC – 0.380). R^2 values for AC (0.920) and Ca-AC (0.822) indicated a favourable adsorption process using the pseudo-second-order kinetic model. The rate of adsorption decreased as the initial dye concentration increased (20–80 mg l^{-1}). For AC (0.929) and Ca-AC (0.938), the intraparticle diffusion model was the rate-limiting step. The rate of adsorption was found to decrease for coconut husk activated carbon[36], salvia seeds[38] and papaya seed powder[39]. Table 4 compares different adsorbents used for malachite green dye removal.

Adsorption mechanism

Different factors such as solution film surrounding diffusion or surface internal site diffusion influence the rate of adsorption. The uptake can also be controlled by mechanisms such as ion exchange, complexation, diffusion and precipitation.

The kinetics of malachite green dye on the surface of AC and Ca-AC is primarily governed by the diffusion process. The curve initially reflects surface adsorption and external surface diffusion, but the process eventually indicates gradual internal mass transfer and intraparticle diffusion in the final stage[40]. Intraparticle diffusion is the rate-limiting step for the adsorption of malachite dye on AC (0.929) and Ca-AC (0.938).

Conclusion

Agricultural waste products have the potential to be utilized as low-cost adsorbents for the effective removal and recovery of pollutants from wastewater. In this study, the adsorption of malachite green dye on AC was examined in-depth. The characterization of AC through BET, FTIR and TGA/DSC revealed that it had desirable morphological properties for adsorption. The findings showed that activation with calcium carbonate led to an enhancement in pore formation and surface area, resulting in more efficient multilayer adsorption of malachite green dye on the surface of Ca-AC (40.35 mg g^{-1}). Additionally, the study found that coconut shells can serve as an effective adsorbent for dye removal from real industrial effluents and could be a cost-effective alternative to commercial AC. To further develop this technology, future research can focus on scaling-up the process to make filters from lignocellulosic biomass.

Conflict of interest: The authors declare that there is no conflict of interest.

1. Putro, J. N., Ju, Y.-H., Soetaredjo, F. E., Santoso, S. P. and Ismadji, S., In *Biosorption of Dyes*, Elsevier, 2021, pp. 99–133; https://doi.org.10.1016/B978-0-012-817-742-6.00004-9.
2. Sadiq, A. C., Rahim, N. Y. and Suah, F. B. M., Adsorption and desorption of malachite green by using chitosan–deep eutectic solvents beads. *Int. J. Biol. Macromol.*, 2020, **164**, 3965–3973; doi:10.1016/j.ijbiomac.2020.09.029.
3. Man, L. W., Kumar, P., Teng, T. T. and Wasewar, K. L., Design of experiments for malachite green dye removal from wastewater using thermolysis – coagulation–flocculation. *Desalin. Water Treat.*, 2012, **40**(1–6), 260–271; doi:10.1080/19443994.2012.671257.
4. Mourão, P. A. M., Laginhas, C., Custódio, F., Nabais, J. M. V., Carrott, P. J. M. and Carrott, M. M. L. R., Influence of oxidation process on the adsorption capacity of activated carbons from lignocellulosic precursors. *Fuel Process. Technol.*, 2011, **92(**2), 241–246; doi:10.1016/j.fuproc.2010.04.013.
5. Kuzniatsova, T. A., Mottern, M. L., Chiu, W. V., Kim, Y., Dutta, P. K. and Verweij, H., Synthesis of thin, oriented zeolite A membranes on a macroporous support. *Adv. Funct. Mater.*, 2008, **18**(6), 952–958; doi:10.1002/adfm.200701001.
6. Piriya, R. S., Jayabalakrishnan, R. M., Maheswari, M., Boomiraj, K. and Oumabady, S., Comparative adsorption study of malachite green dye on acid-activated carbon. *Int. J. Environ. Anal. Chem.*, 2020, 1–15; doi:10.1080/03067319.2020.1849667.
7. Obeng, G. Y., Amoah, D. Y., Opoku, R., Sekyere, C. K. K., Adjei, E. A. and Mensah, E., Coconut wastes as bioresource for sustainable energy: quantifying wastes, calorific values and emissions in Ghana. *Energies*, 2020, **13**(9), 2178; doi:10.3390/en13092178.
8. Kabir Ahmad, R., Anwar Sulaiman, S., Yusup, S., Sham Dol, S., Inayat, M. and Aminu Umar, H., Exploring the potential of coconut shell biomass for charcoal production. *Ain Shams Eng. J.*, 2022, **13**(1), 101499; doi:10.1016/j.asej.2021.05.013.
9. Kovács, K. L. *et al.*, Improvement of biogas production by bioaugmentation. *Biomed. Res. Int.*, 2013, **2013**; doi:10.1155/2013/482653.
10. Oumabady, S. *et al*., Application of sludge-derived KOH-activated hydrochar in the adsorptive removal of orthophosphate. *RSC Adv.*, 2021, **11**(12), 6535–6543.
11. Choudhary, M., Kumar, R. and Neogi, S., Activated biochar derived from *Opuntia ficus*-indica for the efficient adsorption of malachite green dye, Cu^{+2} and Ni^{+2} from water. *J. Hazard. Mater.*, 2020, **392**, 122441; doi:10.1016/j.jhazmat.2020.122441.
12. Ekpete, O. A., Harcourt, P., Chemistry, I. and Harcourt, P., Kinetic sorption study of phenol onto activated carbon derived from fluted pumpkin stem waste (*Telfairia occidentalis* Hook F). *ARPN J. Eng. Appl. Sci*., 2011, **6**, 43–49.
13. Xiao, K., Liu, H., Li, Y., Yang, G., Wang, Y. and Yao, H., Excellent performance of porous carbon from urea-assisted hydrochar of orange peel for toluene and iodine adsorption. *Chem. Eng. J.*, 2020, **382**, 122997; doi:10.1016/j.cej.2019.122997.
14. Karthikeyan, S. and Sivakumar, P., The effect of activating agents on the activated carbon prepared from *Feronia limonia* (L.) swingle (wood apple) shell. *J. Environ. Nanotechnol.*, 2012, **1**(1), 05–12; doi:10.13074/jent.2012.10.121009.
15. Thanarasu, A., Periyasamy, K., Manickam Periyaraman, P., Devaraj, T., Velayutham, K. and Subramanian, S., Comparative studies on adsorption of dye and heavy metal ions from effluents using eco-friendly adsorbent. In Materials Today: Proceeding, Elsevier, 2019, pp. 775–781; doi:10.1016/j.matpr.2020.07.001.
16. Kuzniatsova, T. A., Mottern, M. L., Chiu, W. V., Kim, Y., Dutta, P. K. and Verweij, H., Synthesis of thin, oriented zeolite A membranes on a macroporous support. *Adv. Funct. Mater.*, 2008, **18(**6), 952–958; doi:10.1002/adfm.200701001.
17. Hijab, M., Saleem, J., Parthasarathy, P., Mackey, H. R. and McKay, G., Two-stage optimisation for malachite green removal using activated date pits. *Biomass Convers. Biorefin.*, 2020; doi:10.1007/s13399-020-00813-y.
18. Devens, K. U., Neto, S. P., Oliveira, D. L. D. A. and Gonçalves, M. S., Characterization of biochar from green coconut shell and orange peel wastes. *Rev. Virtual Quim.*, 2018, **10**(2), 288–294; doi:10.21577/1984-6835.20180022.
19. Ekpete, O. A., Marcus, A. C. and Osi, V., Preparation and characterization of activated carbon obtained from plantain (*Musa paradisiaca*) fruit stem. *J. Chem.*, 2017; doi:10.1155/2017/8635615.
20. Yorgun, S., Yıldız, D. and Şimşek, Y. E., Activated carbon from *Paulownia* wood: yields of chemical activation stages. *Energy Sources, Part A*, 2016, **38(**14), 2035–2042; doi:10.1080/15567036.2015.1030477.
21. Mozammel, H. M., Masahiro, O. and Bhattacharya, S. C., Activated charcoal from coconut shell using $ZnCl_2$ activation. *Biomass Bioenergy*, 2002, **22**(5), 397–400; doi:10.1016/S0961-9534(02)00015-6.
22. Zawadzki, J., Azambre, B., Heintz, O., Krztoń, A. and Weber, J., IR study of the adsorption and decomposition of methanol on carbon surfaces and carbon-supported catalysts. *Carbon NY*, 2000, **38**(4), 509–515; doi:10.1016/S0008-6223(99)00130-X.
23. Mohan, D. and Singh, K. P., Single- and multi-component adsorption of cadmium and zinc using activated carbon derived from bagasse – an agricultural waste. *Water Res.*, 2002, **36**(9), 2304–2318; doi:10.1016/S0043-1354(01)00447-X.
24. Al-Musawi, T. J., Arghavan, S. M. A., Allahyari, E., Arghavan, F. S., Othmani, A. and Nasseh, N., Adsorption of malachite green dye onto almond peel waste: a study focusing on application of the ANN approach for optimization of the effect of environmental parameters. *Biomass Convers. Biorefin.*, 2022, **1**, 1–12; doi:10.1007/s13399-021-02174-6.

25. Dahri, M. K., Kooh, M. R. R. and Lim, L. B. L., Water remediation using low cost adsorbent walnut shell for removal of malachite green: equilibrium, kinetics, thermodynamic and regeneration studies. *J. Environ. Chem. Eng.*, 2014, **2**(3), 1434–1444; doi:10.1016/j.jece.2014.07.008.
26. Hamzezadeh, A., Rashtbari, Y., Afshin, S., Morovati, M. and Vosoughi, M., Application of low-cost material for adsorption of dye from aqueous solution. *Int. J. Environ. Anal. Chem.*, 2020; doi:10.1080/03067319.2020.1720011.
27. Sartape, A. S., Mandhare, A. M., Jadhav, V. V., Raut, P. D., Anuse, M. A. and Kolekar, S. S., Removal of malachite green dye from aqueous solution with adsorption technique using *Limonia acidissima* (wood apple) shell as low cost adsorbent. *Arab. J. Chem.*, 2017, **10**, S3229–S3238; doi:10.1016/j.arabjc.2013.12.019.
28. Gupta, N., Kushwaha, A. K. and Chattopadhyaya, M. C., Application of potato (*Solanum tuberosum*) plant wastes for the removal of methylene blue and malachite green dye from aqueous solution. *Arab. J. Chem.*, 2016, **9**, S707–S716; doi:10.1016/j.arabjc.2011.07.021.
29. Boudrahem, F., Aissani-Benissad, F. and Aït-Amar, H., Batch sorption dynamics and equilibrium for the removal of lead ions from aqueous phase using activated carbon developed from coffee residue activated with zinc chloride. *J. Environ. Manage.*, 2009, **90**(10), 3031–3039; doi:10.1016/j.jenvman.2009.04.005.
30. Guo, S. *et al.*, Effects of CO_2 activation on porous structures of coconut shell-based activated carbons. *Appl. Surf. Sci.*, 2009, **255**(20), 8443–8449; doi:10.1016/j.apsusc.2009.05.150.
31. Tan, I. A. W., Ahmad, A. L. and Hameed, B. H., Preparation of activated carbon from coconut husk: optimization study on removal of 2,4,6-trichlorophenol using response surface methodology. *J. Hazard. Mater.*, 2008, **153**(1–2), 709–717; doi:10.1016/j.jhazmat.2007.09.014.
32. Chatterjee, R. *et al.*, Effect of pyrolysis temperature on physicochemical properties and acoustic-based amination of biochar for efficient CO_2 adsorption. *Front. Energy Res.*, 2020, **8**, 85; doi:10.3389/fenrg.2020.00085.
33. Brennan Pecha, M., Arbelaez, J. I. M., Garcia-Perez, M., Chejne, F. and Ciesielski, P. N., Progress in understanding the four dominant intra-particle phenomena of lignocellulose pyrolysis: chemical reactions, heat transfer, mass transfer, and phase change. *Green Chem.*, 2019, **21**(11), 2868–2898; doi:10.1039/c9gc00585d.
34. Castro, J. P. *et al.*, Massaranduba sawdust: a potential source of charcoal and activated carbon. *Polymers (Basel)*, 2019, **11**(8); doi:10.3390/polym11081276.
35. Al-Musawi, T. J., Mahvi, A. H., Khatibi, A. D. and Balarak, D., Effective adsorption of ciprofloxacin antibiotic using powdered activated carbon magnetized by iron(III) oxide magnetic nanoparticles. *J. Porous Mater.*, 2021, **28**(3), 835–852; doi:10.1007/s10934-021-01039-7.
36. Bello, O. S., Moshood, M. A., Ewetumo, B. A. and Afolabi, I. C., Ibuprofen removal using coconut husk activated biomass. *Chem. Data Collect.*, 2020, **29**, 100533; doi:10.1016/j.cdc.2020.100533.
37. Afshin, S. *et al.*, Removal of basic blue-41 dye from water by stabilized magnetic iron nanoparticles on clinoptilolite zeolite. *Rev. Chim.*, 2020, **71**(2), 218–229; doi:10.37358/RC.20.2.7919.
38. Alipour, M. *et al.*, Optimising the basic violet 16 adsorption from aqueous solutions by magnetic graphene oxide using the response surface model based on the Box–Behnken design. *Int. J. Environ. Anal. Chem.*, 2019, **101**, 758–777; doi:10.1080/03067319.2019.1671378.
39. Pavan, F. A., Camacho, E. S., Lima, E. C., Dotto, G. L., Branco, V. T. A. and Dias, S. L. P., Formosa papaya seed powder (FPSP): preparation, characterization and application as an alternative adsorbent for the removal of crystal violet from aqueous phase. *J. Environ. Chem. Eng.*, 2014, **2**(1), 230–238; doi:10.1016/j.jece.2013.12.017.
40. Pan, S. Y., Syu, W. J., Chang, T. K. and Lee, C. H., A multiple model approach for evaluating the performance of time-lapse capsules in trapping heavy metals from water bodies. *RSC Adv.*, 2020, **10**(28), 16490–16501; doi:10.1039/d0ra03017a.
41. Sevim, F., Lacin, O., Ediz, E. F. and Demir, F., Adsorption capacity, isotherm, kinetic and thermodynamic studies on adsorption behavior of malachite green onto natural red clay. *Environ. Prog. Sustain. Energy*, 2020, **40**, e13471; doi:10.1002/ep.13471.
42. Xing, Y. and Wang, G., Poly(methacrylic acid)-modified sugarcane bagasse for enhanced adsorption of cationic dye. *Environ. Technol.*, 2009, **30**(6), 611–619; doi:10.1080/09593330902838098.

ACKNOWLEDGEMENTS. We thank the Department of Science and Technology-Science and Engineering Research Board (DST-SERB), New Delhi for financial assistance (sanction number EEQ/000807/2016). We also thank the Department of Environmental Sciences, Tamil Nadu Agricultural University, Coimbatore for help.

Received 12 February 2022; revised accepted 19 January 2023

doi: 10.18520/cs/v124/i10/1167-1174